

M.H. Doall · J.R. Strickler · D.M. Fields · J. Yen

## Mapping the free-swimming attack volume of a planktonic copepod, *Euchaeta rimana*

Received: 28 July 2000 / Accepted: 26 September 2001 / Published online: 16 November 2001  
© Springer-Verlag 2001

**Abstract** The ability of planktonic copepods to detect and pursue remote prey is well documented, but there are no empirical descriptions of their three-dimensional (3D) sensory fields. In this study, the attack volume of females of *Euchaeta rimana* Bradford, a planktonic calanoid copepod, was mapped by plotting the positions of attacked prey within a standardized 3D coordinate system defined by the body axes of *E. rimana*. This analysis was performed using videotaped observations of predatory interactions between free-swimming *E. rimana* and smaller copepod species. Attack by *E. rimana* was an oriented response, accurately directed toward remote prey within an ellipsoidal volume

anterior to its paired first antennules. This attack volume enveloped the large mechanosensory setae projecting anteriorly from the first antennules, with attack distances averaging 1.5 mm, or less than one body length of the predator. *E. rimana* attacked a larger prey species, *Acartia fossae*, at significantly longer distances than it attacked a smaller species, *Acrocalanus inermi*, reflecting prey-specific perceptive volumes. Such perceptual biases may underlie the selective feeding patterns observed in *E. rimana* and other copepod species. These observations are consistent with mechanosensory mechanisms of prey identification and localization, suggesting that fluid disturbances provide the releasing and directing stimuli for *E. rimana* during predatory interactions. Electronic supplementary material to this paper can be obtained by using the Springer LINK server located at <http://dx.doi.org/10.1007/s00227-001-0735-z>.

---

Communicated by J.P. Grassle, New Brunswick

---

Electronic supplementary material to this paper can be obtained by using the Springer LINK server located at <http://dx.doi.org/10.1007/s00227-001-0735-z>.

---

M.H. Doall (✉) · D.M. Fields · J. Yen  
Marine Science Research Center,  
State University of New York at Stony Brook,  
Stony Brook, NY 11794-5000, USA

E-mail: [mdoall@life.bio.sunysb.edu](mailto:mdoall@life.bio.sunysb.edu)  
Tel.: +1-631-6321523  
Fax: +1-631-6327626

J.R. Strickler  
WATER Institute,  
University of Wisconsin-Milwaukee,  
Milwaukee, WI 53208, USA

*Present address:* M.H. Doall  
Department of Ecology and Evolution,  
State University of New York at Stony Brook,  
Stony Brook, NY 11794-5245, USA

*Present address:* D.M. Fields  
School of Biology,  
Georgia Institute of Technology,  
Atlanta, GA 30332, USA

*Present address:* J. Yen  
School of Biology,  
Georgia Institute of Technology,  
Atlanta, GA 30332, USA

---

### Introduction

A growing number of visual observations demonstrate that copepods detect and orient responses toward remote goals, including food items such as algal cells and small zooplankton, as well as mates (Katona 1973; Kerfoot 1978; Alcaraz et al. 1980; Jonsson and Tiselius 1990; Doall et al. 1998). Although light is critical for guiding certain behaviors such as diel vertical migrations (Ringelberg 1999), mechanoreception and chemoreception generally are considered to be the principal sensory modalities used by most copepods in locating target organisms (Mauchline 1998). Morphological and neurological studies indicate the presence of numerous mechanical and chemical receptors on the first antennules of planktonic copepods (Strickler and Bal 1973; Friedman and Strickler 1975; Friedman 1980; Yen et al. 1992; Lenz and Yen 1993). However, their exact sensory-behavioral mechanisms of identification and localization are often difficult to discern due to the complexities of observing these small crustaceans in their three-dimensional (3D) fluid environment.

In the subtropical species *Euchaeta rimana*, both neurophysiological (Yen et al. 1992; Lenz and Yen 1993) and behavioral (Yen and Fields 1994) responses have been elicited by controlled fluid displacements. The paired antennules of *E. rimana* show profound differences between males and females in the number and location of mechano- and chemosensors (Boxshall et al. 1997). Antennules of the non-feeding males are dominated by chemoreceptors, presumably for detecting female pheromones, while female antennules are dominated by mechanoreceptors, presumably for detecting mobile prey. This presumption is supported by feeding studies that show higher clearance rates on active than inactive prey by females of several *Euchaeta* species (Yen 1982, 1985, 1987, 1991). In the middle sectors of female antennules, mechanosensory setae are oriented in a 3D array, perhaps facilitating signal reception within their ambit (Yen and Nicoll 1990).

Here, we observed and analyzed the attack response of free-swimming females of *E. rimana* feeding on smaller copepod species. The relative frequency and success of this crucial behavior influences the feeding rates of copepods on different prey types, and underlies the trophic impact of copepod populations on aquatic ecosystems. In particular, we focused on the spatial parameters over which *E. rimana* attacks prey, taking into account the 3D nature of this copepod's habitat. In the plankton, every direction is accessible to copepods, and sources of signals must be located in three dimensions. Following the reactive distance approach of Holling (1966), we mapped the attack volume of *E. rimana* by plotting the positions of attacked prey around a standard 3D orientation of *E. rimana*. This attack volume, we suggest, reflects a sensory region around *E. rimana* with a range and geometry governed by the copepod's mechanisms of prey detection. Previous descriptions of attack fields of planktonic copepods have been limited to a single two-dimensional (2D) plane, with narrow observation volumes minimizing distances in the third dimension (Kerfoot 1978; Jonsson and Tiselius 1990). We also analyzed the direction of attack relative to prey location to assess the ability of *E. rimana* to localize remote prey.

## Materials and methods

### Copepod collection and maintenance

The predatory copepod *Euchaeta rimana* Bradford was collected 2 km outside Kaneohe Bay, Oahu, Hawaii, towing a 333  $\mu\text{m}$  mesh, 1 m diameter net from 100 m to the surface (Yen 1988). The two prey species, *Acartia fossae* and *Acrocalanus inermis*, were collected in Kaneohe Bay near Coconut Island, using a 110  $\mu\text{m}$  mesh, 0.5 m diameter plankton net. The copepods were transferred to 4-l jars of filtered seawater and hand-carried in thermally insulated containers to J.R. Strickler's laboratory at the University of Southern California. Videotaped observations were made by J. Yen during three separate 10 day periods between August 1986 and February 1987, with freshly captured copepods transported before each round of experiments. Copepods were kept at 20°C, and *E. rimana* was

maintained on a diet of the smaller copepods. Copepods collected with a plankton net off a pier in Long Beach, California, and *Artemia* sp. nauplii hatched in the laboratory were offered to *E. rimana* as a supplement to transported prey.

### Observations and video review

Predatory interactions were recorded at high magnification using a HeNe laser-illuminated, video-tracking system (Strickler 1985). The optical design was described by Strickler and Hwang (1999). Basically, copepods, as well as suspended particles such as phytoplankton, were considered phase objects in a matched, spatial filtering system rendering white silhouettes of the objects against a black background. The light energy of the red laser (0.1 mW cm<sup>-2</sup>) had no observed effect on the swimming behavior of *E. rimana* as compared to that in dim light. Two perpendicularly mounted black/white video cameras were used to record orthogonal views, representing the  $x$ - $z$  and  $y$ - $z$  planes, onto separate video recorders at 60 fields s<sup>-1</sup>, thereby providing a temporal resolution of 16.7 ms. To synchronize the two video-recordings, a time-code generator was used to stamp matching time codes on corresponding video fields. To maintain individual copepods within the fields of view (14×10.5 mm) of the two cameras, the filming vessel was moved in the  $z$ -direction, while the entire optical system was moved in the  $x$ - and  $y$ -directions. The filming vessel (1.1 l) was placed on a vertical linear translator allowing adjustment via a pulley, and was moved with smooth continuous motions to minimize internal water motions. No secondary currents were detected on the basis of tracing suspended particles. The optical system was mounted on an optical breadboard sitting on a pair of linear translators allowing smooth adjustments in the  $x$ - $y$  plane. One liter of glass-fiber filtered seawater was added to the filming vessel, which had the following inner dimensions: 9 × 9 × 14.5 cm (length × width × height).

Both males and females of *E. rimana* were added to the vessel, but the behaviors analyzed here are of females only. Females were easily distinguished from the males by their size, shape, and swimming behavior. Observations were made using a variety of potential prey. *Acartia fossae* and *Acrocalanus inermis* were the prey species for most of the observation time (17 h), with mixtures of adults and copepodites being added. A mix of copepods from Long Beach (2 h observation), and laboratory-hatched *Artemia* sp. nauplii (2 h observation) also were offered as prey in separate experiments. In the two predatory events captured on video using Long Beach copepods as prey, the prey species was *Corycaeus* sp. The concentrations of *E. rimana* and prey were not kept constant between observation periods, with 10–20 *E. rimana* and 20–60 prey added per experiment. To make sure that behaviors were representative, different groups of females of *E. rimana* were used in each experiment. Attacks analyzed here were from 12 different observation periods, assuring that the data are from at least 12 different females.

The normal swimming behaviors of females of *E. rimana* (i.e. not involving interactions with other copepods) were qualitatively described from the 21 h of videotaped observations. All behavioral reactions of *E. rimana* to individual prey were noted and classified as either attack or escape. Attack was defined as a quick lunge by *E. rimana* toward the prey, resulting in either capture of the prey or prey escape, while escapes involved lunges or longer bursts of swimming by *E. rimana* away from a potential prey. Attacks were categorized based upon the prey species, and the success or failure of capture. The capture efficiency of *E. rimana* on each prey type was computed as the number of captures divided by the number of attacks. A total of 34 attack events were recorded and analyzed.

For spatial analysis of predator-prey interactions, individual fields of video were digitally recorded onto an IBM-compatible PC with a model VP1100-640-U-AT overlay frame grabber board (Imaging Technology, Bedford, Mass.), capable of digitizing standard video images at 640 × 480 pixels with 8 bits of pixel depth. The image-analysis software package Optimus (Media Cybernetics, Silver Spring, Md.) was used to spatially calibrate images from pixels into real distances (mm) based on recordings of rulers in the

filming vessel. This software then was used to obtain the spatially calibrated Cartesian positions of seven key reference points in predator–prey systems at the start and end of attack events. Four reference points from *E. rimana* were required to rotate predator–prey systems to the standard 3D orientation, including the: (1) rostrum, (2) distal tips of the paired first antennules (two points), and (3) posterior end of the prosome. In order to define the trajectory of the attack lunge (see Fig. 1), the position of the rostrum of *E. rimana* at the end of the attack lunge was rotated to the standard 3D orientation. The position of the prey was taken at two points: the rostrum and the posterior end of the prosome. The attack volume of *E. rimana* was mapped using the rostrum positions of prey at the initiation of attack.

#### Attack volume

Since the body orientation of *E. rimana* within the “space-constant” coordinate system (i.e. with reference to the outside world; Schöne 1984) varied between attack events, it was necessary to reorient *E. rimana* and prey in each attack event to a “copepod-constant” coordinate system. In the space-constant coordinate system, the vertical axis (i.e. in the opposite direction to gravity) was labeled as  $z$ -, and the  $x$ - and  $y$ -axes formed the horizontal plane. The axes of the copepod-constant coordinate system are parallel to the three main body axes of *E. rimana* (Schöne 1984). The rostro-caudal body axis is the  $X$ -axis; the left–right body axis is the  $Y$ -axis; and the dorso-ventral body axis is the  $Z$ -axis. To distinguish the two coordinate systems, space-constant axes were denoted using small-case letters and copepod-constant axes were labeled with capital letters. The rostrum position of *E. rimana* was designated as the origin for both coordinate systems. The rostrum is midway between the paired first antennules, the most conspicuous sensory organ of *E. rimana*, and is close to the capture region where prey may be grasped by the maxillipeds.

Three consecutive 2D rotations (one for each 2D plane) were performed, each around the initial rostrum position of *E. rimana* (i.e.  $x=0$ ,  $y=0$ ,  $z=0$ ). In the first rotation, the  $x$ - and  $z$ -axes were rotated so that the posterior end of *E. rimana*'s prosome was positioned at  $z'=0$ . The angle of rotation as well as the new coordinates of each reference point following the rotation were computed from the equations for rotation of axes (Swokowski 1988):

$$x' = x \cos(q) + z \sin(q) \quad (1)$$

$$z' = -x \sin(q) + z \cos(q) \quad (2)$$

where  $q$  is the angle of rotation,  $x$  and  $z$  are the coordinates of point  $P$  before rotation, and  $x'$  and  $z'$  are the coordinates of point  $P$  after rotation. The angle of rotation was computed first from Eq. 2, in which  $x$  and  $z$  were known and  $z'$  was set to 0. After solving for  $q$ ,  $x'$  was computed from Eq. 1. In the second rotation, the  $x$ - and  $y$ -axes were rotated so that the posterior end of the prosome was positioned at  $y'=0$ . The same procedure described above was used, replacing  $z$  and  $z'$  with  $y$  and  $y'$ , respectively, in the equations. Finally, the  $y$ - and  $z$ -axes were rotated so that the two distal tips of the first antennae of *E. rimana* were positioned at the same  $z$ -coordinate. To perform this rotation, the straight line connecting the two distal tips was considered the hypotenuse of a right triangle, and  $q$  was computed from the following equation:

$$\tan(q) = \frac{z \text{ distance between distal tips}}{y \text{ distance between distal tips}} \quad (3)$$

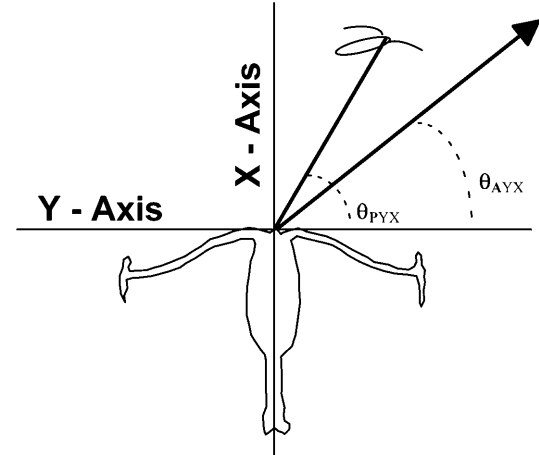
After solving for  $q$ ,  $y'$  and  $z'$  were computed from Eqs. 1 and 2, in which  $x$  and  $x'$  were replaced with  $y$  and  $y'$ , respectively. Following the three rotations, the space-constant coordinate axes were aligned with the copepod-constant coordinate axes.

Distances, including prosome lengths, were calculated using  $X$ ,  $Y$ ,  $Z$  coordinates. Attack distances were computed as the distance between the rostrum positions of *E. rimana* and the prey. The prosome lengths of predator and prey in each attack event were

computed as the distance between the rostrum and the posterior end of the prosome.

*Acartia fossae* was the prey species in 22 of the 34 attacks, *Acrocalanus inermis*, the prey in nine attacks, *Corycaeus* sp., the prey in two attacks, and *Artemia* sp., the prey in one attack. Limited sample sizes prevented comparisons between all prey species, so only *A. fossae* and *A. inermis* were compared. Two-tailed  $t$ -tests were used to compare prosome lengths and attack distances between the two prey species. A  $G$ -test for independence was used to compare the capture efficiencies of *E. rimana* on the two prey species. An alpha level of 0.05 was used to determine significance in all statistical tests.

#### A. Y-X Plane



#### B. Z-X Plane

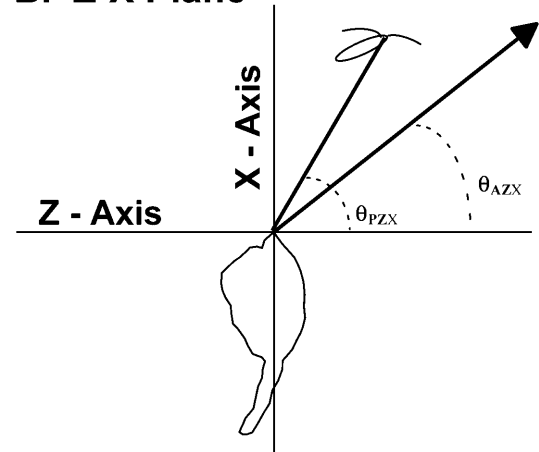


**Fig. 1a, b** *Euchaeta rimana*. Copepod-constant orientation of predator–prey systems from  $Y$ – $X$  planar view (**a**) and  $Z$ – $X$  planar view (**b**). **a** Ventral surface of *E. rimana* viewed, and entire length of first antennae can be seen. Angle of attack lunge ( $\theta_{AYX}$ ) measured between trajectory of *E. rimana*'s rostrum and positive  $Y$ -axis. Angle of prey location ( $\theta_{PYX}$ ) measured between straight line connecting *E. rimana* to prey (rostrum to rostrum) and positive  $Y$ -axis. Angles are positive when measured counterclockwise from positive  $Y$ -axis, and negative when measured clockwise from positive  $Y$ -axis. **b** Lateral surface of *E. rimana* viewed with ventral surface facing to left, and first antennae directed into and out of the plane. Angles the same as in panel a, but measured from the positive  $Z$ -axis

## Attack lunge

The trajectory of the attack lunge was defined by the straight line connecting the initial and final rostrum positions of *E. rimana* (Fig. 1). The final rostrum position was digitized following deceleration of the attack lunge, between two to three video fields (33.3–50 ms) after the initiation of attack. Therefore, computed lunge velocities underestimated maximum lunge velocities since they incorporated the decelerating phase of the attack lunge. The velocities of prey during escape responses were computed in the same way.

The angle of the attack lunge ( $\theta_A$ ) was measured between the trajectory of the lunge and the positive horizontal axis in both the  $Y$ - $X$  plane (Fig. 1a) and  $Z$ - $X$  plane (Fig. 1b). The angle of attack increased from  $0^\circ$  (i.e. positive horizontal axis) to  $180^\circ$  (i.e. negative horizontal axis) arcing in a counterclockwise direction from the positive horizontal axis, and from  $0^\circ$  to  $-180^\circ$  in a clockwise direction. Thus, all attacks directed anteriorly had a positive lunge angle, and all attacks directed posteriorly had a negative lunge angle. The angle of prey location ( $\theta_P$ ) in the  $Y$ - $X$  and  $Z$ - $X$  planes was measured between the straight line connecting *E. rimana* to prey (rostrum to rostrum) and the positive horizontal axis. The ability of *E. rimana* to locate prey and direct its attack lunge was assessed through comparison of  $\theta_A$  and  $\theta_P$  in separate attacks. If *E. rimana* directs its attack response in three dimensions toward prey locations, we expected  $\theta_A$  and  $\theta_P$  to have a 1:1 relationship in both the  $Y$ - $X$  and  $Z$ - $X$  planes.

## Results

### Normal swimming behavior

While searching for prey, the swimming style of *Euchaeta rimana* varied with its speed. At slower speeds (i.e.  $< 3 \text{ mm s}^{-1}$ ), the motion of females was described as “hovering” (video 1, electronic supplementary material). During hovering, *E. rimana* glided slowly or remained nearly stationary, with its rostro-caudal body axis vertical (i.e. opposite to gravity) as it generated an anterior feeding current to entrain prey. Hovering females moved slowly up or down in the water column, as well as horizontally. Despite horizontal components to velocity, the rostro-caudal body axis remained vertical during hovering. During both horizontal and vertical movement, a hovering *E. rimana* often rotated around its rostro-caudal body axis. Hovering was occasionally interrupted by turns toward one side, during which the copepod dropped into a horizontal orientation (ventral side facing down), sinking slightly in the process. This maneuver, which lasted  $< 66 \text{ ms}$ , involved use of the swimming legs and first antennules. Following the turn, the horizontally oriented copepod swam antero-dorsally, curving up into a vertical position to resume hovering.

At higher speeds, ranging up to  $13 \text{ mm s}^{-1}$ , swimming was better described as “cruising”, and a feeding current that entrained prey was not evident (video 2, electronic supplementary material). Rather, the rostro-caudal axis was oriented in the direction of motion, so that the anteriorly projecting setae of the paired first antennules were the first section of the body to enter new, undisturbed water. The rostro-caudal axis was oriented horizontally, with the ventral surface facing down during

horizontal movement, and was vertical during upward or downward swimming. Looping and turning often were exhibited during cruising. During looping behavior, the copepod curved in an antero-dorsal direction, often completing multiple loops in a spiraling pattern.

The two swimming styles were not always distinct, with a combination of hovering and cruising at intermediate velocities. Propulsion for both swimming styles was accomplished with high-frequency motions of the cephalic appendages, particularly the second antennae, and did not include strokes of the swimming legs. Prey were remotely detected and successfully attacked and captured by *E. rimana* during both hovering (video 3, electronic supplementary material) and cruising (video 4, electronic supplementary material), and from both vertical and horizontal body orientations. On several occasions, attack occurred following a turn from a hovering position as the copepod was swimming horizontally. Several attacks were also observed during looping behavior (video 4, electronic supplementary material).

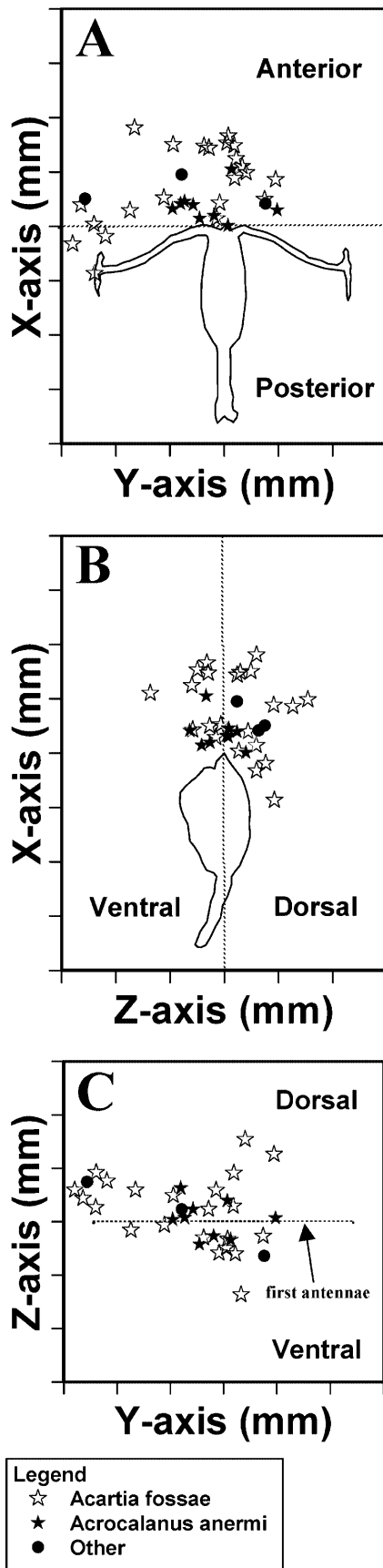
### Escape responses of prey

The feeding current of a hovering *E. rimana* elicited small “hops” in copepods entrained within it. Propulsion for these hops was accomplished through a downward paddle of the swimming legs and first antennules. These hops usually were directed against the flow, and the copepod was often re-entrained in the feeding current several times before either successfully escaping the flow, or eliciting an attack by *E. rimana*. The average hop distance of *Acartia fossae*, traversed within 50 ms, was  $1.63 \pm 0.70 \text{ mm}$  ( $n=6$ ), and the average speed over this distance was  $44.3 \pm 21.3 \text{ mm s}^{-1}$ .

In the first video field of most attacks, a small blur was observed around both predator and prey, indicating that both copepods were in motion, but the temporal resolution was insufficient to tell which individual moved first. Movement by the prey may have been either: (1) a hop elicited in response to the feeding current before *E. rimana* initiated attack, or (2) an escape response elicited after *E. rimana* initiated attack. In some events, however, it was evident that the prey hop commenced one video field (i.e. 16.7 ms) prior to attack, suggesting that these prey motions had produced hydrodynamic disturbances that elicited rapid attack responses by *E. rimana*.

### Attack response

*E. rimana* displayed two characteristic responses to prey – attack and escape. Attacks involved a single rapid lunge by *E. rimana* toward the prey (videos 3 and 4, electronic supplementary material). Escapes, on the other hand, involved single lunges or longer bursts of fast swimming away from the prey. All observed attacks were on



remotely located prey, while most escapes were elicited when prey contacted *E. rimana*, either because they swam into *E. rimana*, or were drawn in by its feeding current.

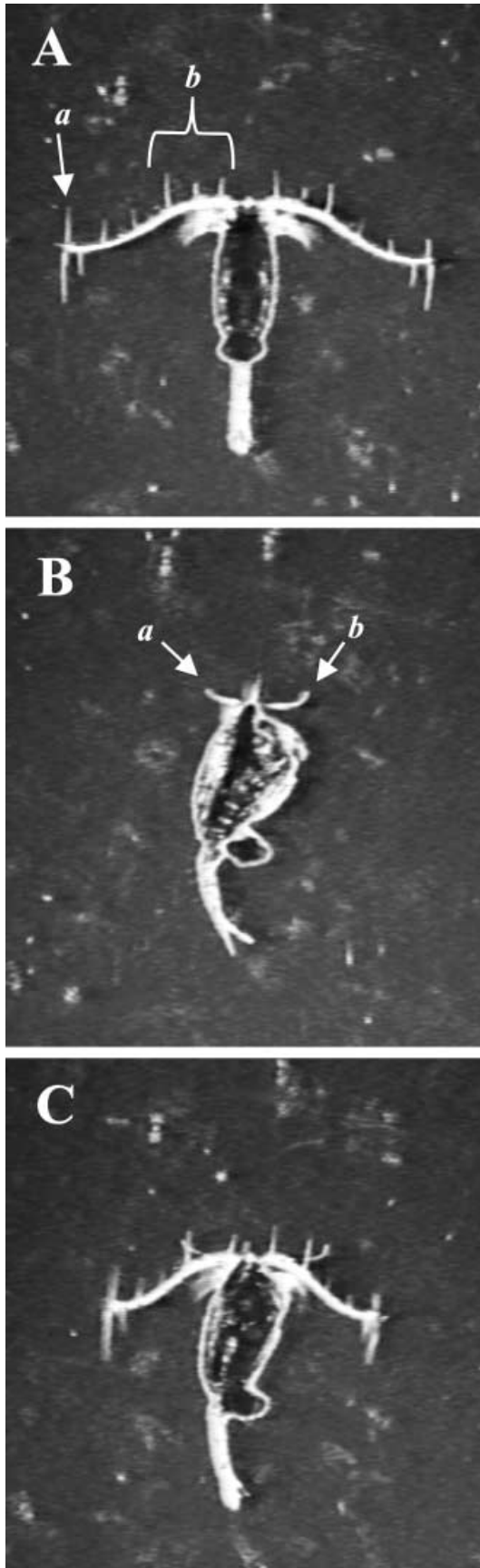
Propulsion for these rapid responses involved: (1) downward sweeps of the swimming legs, (2) flexion of the urosome, and (3) folding of the first antennules along the sides of the body. The temporal resolution of the video recordings was insufficient to describe the sequence of appendage movements. Attacks involved only one power stroke of these swimming appendages, and *E. rimana* covered distances averaging  $3.72 \pm 1.23$  mm (mean  $\pm$  SD; range = 1.48–5.78 mm;  $n = 27$ ) within 50 ms (i.e. three fields of video) after initiation of the attack. The average speed over this distance was  $98.2 \pm 32.9$  mm  $s^{-1}$  (range = 44.5–173.4 mm  $s^{-1}$ ;  $n = 27$ ). If capture was unsuccessful *E. rimana* did not attempt a second attack, resuming its previous searching behavior as the smaller copepod prey rapidly swam away.

Prey were attacked within an ellipsoidal volume centered anterior to the paired first antennules of *E. rimana* (Fig. 2). The longest dimension of this attack volume fell along the *Y*-axis, spanning the length of the first antennules, approximately 2.5 mm lateral to the rostrum in each direction (Fig. 2a). Prey positions were more condensed along the *Z*-axis than the *Y*-axis, with the furthest prey location in the *Z*-direction extending 1.5 mm from the rostrum (Fig. 2b). Prey positions averaged  $0.54 \pm 0.39$  mm (range = 0.04–1.54 mm;  $n = 21$ ) dorsal to *E. rimana* (i.e. along positive *Z*-axis), and  $0.45 \pm 0.33$  mm (range = 0.06–1.37 mm;  $n = 13$ ) ventral to *E. rimana* (i.e. along negative *Z*-axis). Prey were located anterior to the first antennules in all attack events (Fig. 2a). Since the first antennules of *E. rimana* curve posteriorly along their length, three prey locations were anterior to the distal tip of a first antenna but posterior to the rostrum (Fig. 2a). Prey were anterior to the rostrum in all other attacks, with prey positions averaging  $0.76 \pm 0.54$  mm along the positive *X*-axis (range = 0.00–1.81 mm;  $n = 31$ ).

This attack volume enveloped the large mechanosensory setae that project anteriorly from the first antennules of *E. rimana* (Fig. 3). In particular, prey locations clustered around the longest and most prominent setae, including the paired, four-point, setal arrays on the proximal sections of the first antennules, and the setae on one distal tip. We do not interpret the lack of prey locations at the distal tip of the other antennule as

◀

**Fig. 2a–c** *Euchaeta rimana*. Attack volume plotted in three two-dimensional planes: *Y*–*X* plane (a), *Z*–*X* plane (b), and *Y*–*Z* plane (c). Data points are prey locations at initiation of attack lunge, with symbols distinguishing different prey species. Outline of *E. rimana* is average size of adult females observed. **a** Ventral view with entire length of first antennules seen. **b** Lateral view with ventral surface facing left, and first antennules directed into and out of the plane. **c** Anterior view with dashed line representing first antennules, scaled to appropriate length. Above dashed line is volume dorsal to *E. rimana*, and below dashed line is volume ventral to *E. rimana*



reflecting lateral asymmetry in the sensory system, but attribute it to small sample size. Of the six attacks on distally located prey (Fig. 2a), three were by one individual *E. rimana* that appeared to have a damaged seta at the distal tip of one antennule.

The average attack distance within the attack volume was  $1.50 \pm 0.71$  mm (range = 0.38–2.88 mm;  $n = 34$ ), or less than one body length of the predator. *E. rimana* attacked *Acartia fossae* at significantly longer distances than it attacked a smaller species, *Acrocalanus inermi* ( $t = 4.34$ ,  $P < 0.001$ ). Attack distances averaged  $1.76 \pm 0.63$  mm for attacks on *A. fossae*, and  $0.81 \pm 0.29$  for attacks on *A. inermi*. One obvious difference between the prey species was size, with *A. fossae* being significantly larger ( $t = 8.99$ ,  $P < 0.001$ ). The average prosome length of *A. fossae* was  $0.77 \pm 0.09$  mm ( $n = 22$ ), while that of *A. inermi* was  $0.45 \pm 0.08$  mm ( $n = 9$ ). Overall, the prosome lengths of attacked prey ranged from 18% to 44% of the prosome length of the attacking *E. rimana*, which averaged  $2.19 \pm 0.16$  mm.

*E. rimana* directed its attack response in three dimensions toward the location of its prey, being capable of localizing the signals created by prey, and controlling the direction of its attack response. The temporal resolution of standard video recording was insufficient to determine how *E. rimana* controls the direction of its attack lunge. Attack lunges were directed anteriorly for prey anterior to the rostrum, resulting in positive lunge angles (Fig. 4). In the three attack events in which prey were slightly posterior to the rostrum, attack lunges had a small posteriorly directed component, resulting in negative lunge angles (Fig. 4). *E. rimana* was able to localize prey and direct its attack to either side (Fig. 4a). The attack lunge had a dominantly lateral component in attacks on prey in the distal extremes of the attack volume. In several attacks on prey at these extremes, *E. rimana* rotated approximately  $90^\circ$  around its rostro-caudal axis so as to approach the prey dorsal side first, passing below the prey and reaching up with its maxillipeds to capture it. Prey located both dorsal ( $n = 21$ ) and ventral ( $n = 13$ ) to *E. rimana* were attacked. However, the movement of *E. rimana* along the Z-axis during attack was limited to the dorsal direction (i.e. angle of attack between  $0^\circ$  and  $90^\circ$  in the Z–X planar view; Fig. 4b), and attacks on ventrally located prey deviated most from a 1:1 relationship between lunge angle and prey angle in the Z–X plane (Fig. 4b). Despite this deviation, capture efficiency was relatively high (67%) on ventrally located prey. *E. rimana* captured ventrally



**Fig. 3a–c** *Euchaeta rimana*. Schlieren images of female showing array of setal mechanosensors on first antennules. **a** Ventral view with distal seta labeled *a*, and four-point setal array labeled *b*. In the middle of the four-point array are two setae, one that extends dorsally and one ventrally. These two setae overlap in this view and appear as one. **b** Lateral view with dorsally projecting seta of paired four-point array labeled as *a*, and ventrally projecting seta of paired four-point array labeled as *b*. **c** Oblique view

located prey by extending its long maxillipeds outward as it lunged up past the prey.

Overall, prey were captured in 56% of the attacks by *E. rimana*. Capture efficiencies did not differ significantly between attacks on *A. fossae* and *A. inermi*, being 55% and 44%, respectively ( $G=0.25$ ,  $P>0.6$ ). Prey that eluded capture were attacked at an average distance of  $1.71 \pm 0.81$  mm, while those that were successfully captured were attacked at a shorter distance of  $1.34 \pm 0.58$  mm. This difference was not significant ( $t=1.55$ ,  $0.1 < P < 0.2$ ), but may reflect a failure by *E. rimana* to overtake prey when attacking from long distances. Considering the escape and attack speeds of prey and predator, respectively, prey located at the distal extremes of the attack volume may stay out of striking range of an attacking *E. rimana*.

## Discussion

We have mapped the attack volume of freely swimming females of *Euchaeta rimana* based on attacks by this predatory copepod on smaller, mobile copepods. We found that the attack volume of *E. rimana* spatially

matches the distribution of the long mechanosensory setae on its first antennules, providing further evidence that these mechanosensors serve as prey detectors. Prey are most frequently detected near the prominent four-point setal arrays that project anteriorly from the proximal sections of the first antennules, but prey near the large setae at the distal tips of the first antennules may also be attacked. The principal function of the long distal setae previously has been hypothesized to be predator detection due to their location outside of the feeding current of *E. rimana* (Lenz and Yen 1993), but our data indicate that these setae also function in prey detection.

The distances at which prey were attacked by *E. rimana* are consistent with a mechanosensory mechanism, because fluid disturbances at low Reynold's number are short lived. Natural wakes shed by hopping copepods show a rapid decline in velocity within a few millimeters of the copepod (Van Duren et al. 1998; Yen et al. 1998). The effects of hops by *Temora longicornis*, a 1 mm copepod, on the surrounding fluid dissipate after 0.5 s (Van Duren et al. 1998). Within the attack volume of *E. rimana*, prey are never  $> 3$  mm from its rostrum, and even closer to the anteriorly projecting mechanosensory setae. Similar attack distances have been measured for other copepods preying on smaller zooplankton (Kerfoot 1978; Williamson and Vanderploeg 1988; Jonsson and Tiselius 1990).

The distances at which prey are detected can be expected to increase with the force applied to the fluid by the prey. Large prey can be assumed to generate stronger fluid disturbances than small prey, and therefore should be detected at longer distances by predatory copepods. This assumption is supported by our observation that *E. rimana* attacks *Acartia fossae* at longer distances than the smaller copepod *Acrocalanus inermi*. However, we cannot rule out the possibility that this difference in attack distance was due to specific differences in swimming behavior regardless of prey size. Nonetheless, there are correlations between attack distance and prey size for other predatory copepods. The cyclopoid *Cyclops vernalis* attacks large *Chydorus sphaericus* at greater distances than smaller ones (Kerfoot 1978). The omnivorous calanoid *Acartia tonsa* attacks large ciliate species at greater distances than small ciliate species (Jonsson and Tiselius 1990).

Since large prey may be detected at longer distances than small prey by predatory copepods, large prey may be encountered more frequently. In terms of Gerritsen and Strickler's (1977) encounter model, the "encounter radius" of a predatory copepod may increase with prey size. Additionally, swimming speeds usually increase with development and size, further increasing encounter rates. However, larger, more-developed copepods also have more powerful escape capabilities (Landry 1978), potentially reducing the capture efficiencies of their predators. Furthermore, large prey may be more difficult to grasp and handle by the capture appendages. In this study, only preferred prey sizes were offered, so reduced

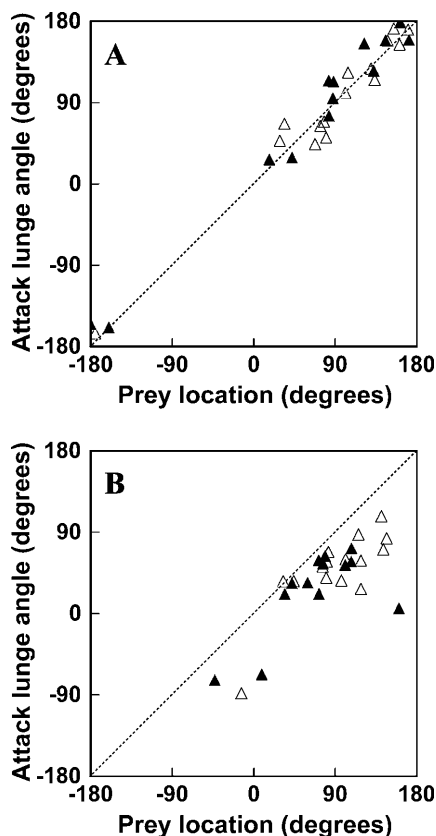


**Fig. 4a, b** *Euchaeta rimana*. Accuracy of attack in  $Y-X$  plane (**a**) and  $Z-X$  plane (**b**). Open triangles are attacks resulting in prey capture. Closed triangles are attacks resulting in prey escape. Line on the graph marks the 1:1 relationship between lunge angle and prey angle

capture efficiency on larger prey could not be observed. We assume that for *E. rimana* the upper limit to prey size is greater than the 0.8 mm prosome length of the largest prey species (*A. fossae*) examined here. Taken together, the balance between encounter rate and capture efficiency may set an optimal prey size for predatory copepods, helping to explain the size-specific patterns of selective predation that have been observed in a number of predatory copepods (Yen 1982, 1985, 1991; Greene and Landry 1985, 1988). Of course, size alone cannot fully account for prey vulnerability. Other factors, such as the swimming behavior and armor of prey, will also influence the rates at which they are encountered and captured.

We observed that attacks by *E. rimana* often are immediately preceded (i.e. < 16.7 ms) by an escape hop of the prey. These escape hops are accomplished through a downward thrust of the swimming legs and first antennules, creating a flow pattern that is very different than that generated during suspension feeding (Kerfoot et al. 1980; Kirk 1985; Yen and Strickler 1996; Van Duren et al. 1998). Kirk (1985) measured much higher velocities and accelerations in the aperiodic pulses of water produced by a hopping *Daphnia pulex* (a cladoceran) than in the steady flow produced by the swimming calanoid *Diatomus hesperus*, which was of comparable size. Van Duren et al. (1998) found a 12-fold increase in the volume of water influenced by the calanoid *Temora longicornis* during hops as compared with foraging. Since thrusts with swimming legs produce the furthest reaching fluid disturbances from copepods, it is reasonable to suspect that this behavior generates important cues to mechanosensory predators. This hypothesis is supported by the experiments of Yen and Fields (1994), in which odorless water jets resembling the wakes of escaping copepods were used to elicit attack in *E. rimana*. Furthermore, Tiselius et al. (1997) observed a higher predation rate on the copepod *Acartia clausi* by the predatory copepod *Pareuchaeta norvegica* under conditions causing *A. clausi* to jump more.

We also found the attack by *E. rimana* to be an oriented response, accurately directed toward remote prey. This attack response is an example of "target orientation", in which a goal (i.e. prey) is attained through a "single brief motor action" (Schöne 1984). Many other prey-capture behaviors throughout the animal kingdom can be classified as target orientations, such as when a praying mantis strikes with its forelegs, or when a snake strikes with its fangs. Unlike most examples of target orientation, however, the attack response of *E. rimana* is not directed through vision. Rather, the setal mechanosensors of copepods appear to provide directional information. The setae along the first antennules are innervated and structurally constrained in the direction of movement, and neurophysiological studies have revealed directional sensitivity in these mechanosensors (Yen et al. 1992). However, the number of mechanosensors that must be excited in order for *E. rimana* to determine direction is unknown. If many sensors are

stimulated, the multi-directed setal array may sample flow direction and intensity along all three planes, permitting localization of prey within 3D space. The temporal pattern of stimulation of different setae and the signal strength at each receptor may also provide important directional information.

In conclusion, we have found that when freely swimming, the predatory copepod *E. rimana* exhibits precise 3D-oriented attack lunges that efficiently capture mobile prey within a volume anterior to the array of setal mechanosensors along the paired antennules. This attack response is an example of a target-oriented behavior in copepods, released and directed through the fluid disturbances created by prey. These fluid disturbances created by millimeter-sized prey dissipate rapidly due to the viscosity of the fluid, and attack lunges consequently are limited to prey located within millimeters of the sensor array. The speed and 3D accuracy of the attack response of *E. rimana* insures capture success in an environment where encountering prey is infrequent, due to the small size of the plankton, their distribution and abundance within the vast open ocean, and the physical limitations to near-field detection.

**Acknowledgements** We gratefully acknowledge the Functional Ecology Research and Training Laboratory (FERTL) in the Department of Ecology and Evolution, SUNY at Stony Brook for providing the computing facilities during the preparation of this manuscript. We thank Dr. D. Padilla and two anonymous reviewers for reviewing and improving our manuscript. This work was funded by NSF grants OCE-9314934 and IBN 97-23960 and ONR contract N000149410696 to J. Yen.

## References

- Alcaraz M, Paffenhöfer G-A, Strickler JR (1980) Catching the algae: a first account of visual observations on filter-feeding calanoids. In: Kerfoot WC (ed) Evolution and ecology of zooplankton communities. University Press of New England, Hanover, N.H., pp 241–248
- Boxshall GA, Yen J, Strickler JR (1997) Functional significance of the sexual dimorphism in the cephalic appendages of *Euchaeta rimana* Bradford. Bull Mar Sci 61:387–398
- Doall MH, Colin SP, Strickler JR, Yen J (1998) Locating a mate in 3D: the case of *Temora longicornis*. Philos Trans R Soc Lond B Biol Sci 353:681–689
- Friedman MM (1980) Comparative morphology and functional significance of copepod receptors and oral structures. In: Kerfoot WC (ed) Evolution and ecology of zooplankton communities. University Press of New England, Hanover, N.H., pp 185–197
- Friedman MM, Strickler JR (1975) Chemoreceptors and feeding in calanoid copepods (Arthropoda: Crustacea). Proc Natl Acad Sci USA 72:4185–4188
- Gerritsen J, Strickler JR (1977) Encounter probabilities and community structure in zooplankton: a mathematical model. J Fish Res Board Can 34:73–82
- Greene CH, Landry MR (1985) Patterns of prey selection in the cruising calanoid predator *Euchaeta elongata*. Ecology 66: 1408–1416
- Greene CH, Landry MR (1988) Carnivorous suspension feeding by the subarctic calanoid copepod *Neocalanus cristatus*. Can J Fish Aquat Sci 45:1069–1074
- Holling CS (1966) The functional response of invertebrate predators to prey density. Mem Entomol Soc Can 48:1–86

- Jonsson PR, Tiselius P (1990) Feeding behavior, prey detection and capture efficiency of the copepod *Acartia tonsa* feeding on planktonic ciliates. *Mar Ecol Prog Ser* 60:35–44
- Katona SK (1973) Evidence for sex pheromones in planktonic copepods. *Limnol Oceanogr* 18:574–583
- Kerfoot WC (1978) Combat between predatory copepods and their prey: *Cyclops*, *Epischura*, and *Bosmina*. *Limnol Oceanogr* 23:1089–1102
- Kerfoot WC, Kellogg DL, Strickler JR (1980) Visual observations of live zooplankters: evasion, escape, and chemical defenses. In: Kerfoot WC (ed) *Evolution and ecology of zooplankton communities*. University Press of New England, Hanover, N.H., pp 10–27
- Kirk KL (1985) Water flows produced by *Daphnia* and *Diaptomus*: implications for prey selection by mechanosensory predators. *Limnol Oceanogr* 30:679–686
- Landry MR (1978) Predatory feeding behavior of a marine copepod, *Labidocera trispinosa*. *Limnol Oceanogr* 23:1103–1113
- Lenz PH, Yen J (1993) Distal setal mechanoreceptors of the first antennae of marine copepods. *Bull Mar Sci* 53:170–179
- Mauchline J (1998) *The biology of calanoid copepods*. Academic, San Diego
- Ringelberg J (1999) The photobehaviour of *Daphnia* spp. as a model to explain diel vertical migration in zooplankton. *Biol Rev Camb Philos Soc* 74:397–423
- Schöne H (1984) *Spatial orientation: the spatial control of behavior in animals and man*. Princeton University Press, Princeton, N.J.
- Strickler JR (1985) Feeding currents in calanoid copepods: two new hypotheses. In: Laverack MS (ed) *Physiological adaptations of marine animals*. The Company of Biologists, Cambridge, pp 459–485
- Strickler JR, Bal AK (1973) Setae of the first antennae of the copepod *Cyclops scutifer* (Sars): their structure and importance. *Proc Natl Acad Sci USA* 70:2656–2659
- Strickler JR, Hwang J-S (1999) Matched spatial filters in long working distance microscopy of phase objects. In: Cheng PC, Hwang PP, Wu JL, Wang G, Kim H (eds) *Focus on multidimensional microscopy*. World Scientific, River Edge, N.J., pp 217–239
- Swokowski EW (1988) *Calculus with analytic geometry*, 2nd alternate edn. PWS-Kent, Boston
- Tiselius P, Jonsson PR, Kaartvedt S, Olsen EM, Jorstad T (1997) Effects of copepod foraging behavior on predation risk: an experimental study of the predatory copepod *Pareuchaeta norvegica* feeding on *Acartia clausi* and *A. tonsa* (Copepoda). *Limnol Oceanogr* 42:164–170
- Van Duren LA, Stamhuis EJ, Videler JJ (1998) Reading the copepod personal ads: increasing encounter probability with hydromechanical signals. *Philos Trans R Soc Lond B Biol Sci* 353:691–700
- Williamson CE, Vanderploeg HA (1988) Predatory suspension-feeding in *Diaptomus*: prey defenses and the avoidance of cannibalism. *Bull Mar Sci* 43:561–572
- Yen J (1982) Sources of variability in attack rates of *Euchaeta elongata* Esterly, a carnivorous marine copepod. *J Exp Mar Biol Ecol* 63:105–117
- Yen J (1985) Selective predation by the carnivorous marine copepod *Euchaeta elongata*: laboratory measurements of predation rates verified by field observations of temporal and spatial feeding patterns. *Limnol Oceanogr* 30:577–597
- Yen J (1987) Predation by a carnivorous marine copepod, *Euchaeta norvegica* Boeck, on eggs and larvae of the North Atlantic cod *Gadus morhua* L. *J Exp Mar Biol Ecol* 112:283–296
- Yen J (1988) Directionality and swimming speeds in predator-prey and male-female interactions of *Euchaeta rimana*, a subtropical marine copepod. *Bull Mar Sci* 43:395–403
- Yen J (1991) Predatory feeding behavior of an Antarctic marine copepod, *Euchaeta antarctica*. In: Sakshaug E, Hopkins CCE, Oritsland NA (eds) *Proceedings of the Pro Mare Symposium on Polar Marine Ecology*. *Polar Res* 10:433–442
- Yen J, Fields DM (1994) Behavioral responses of *Euchaeta rimana* to controlled fluid mechanical stimuli (abstract). *EOS, Trans Am Geophys Un* 75:184
- Yen J, Nicoll NT (1990) Setal array on the first antennae of a carnivorous marine copepod *Euchaeta norvegica*. *J Crustac Biol* 10:218–224
- Yen J, Strickler JR (1996) Advertisement and concealment in the plankton: what makes a copepod hydrodynamically conspicuous? *Invertebr Biol* 115:191–205
- Yen J, Lenz PH, Gassie DV, Hartline DK (1992) Mechanoreception in marine copepods: electrophysiological studies on the first antennae. *J Plankton Res* 14:495–512
- Yen J, Weissburg MJ, Doall MH (1998) The fluid physics of signal perception by mate-tracking copepods. *Philos Trans R Soc Lond B Biol Sci* 353:787–804